Available online at www.elixirpublishers.com (Elixir International Journal)

Applied Mathematics

Elixir Appl. Math. 51 (2012) 10809-10816

ISSN: 2229-712X

Soret and Dufour Effects on Boundary Layer Flow past an Exponential Stretching Sheet with Thermal Radiation and Viscous Dissipation

P. Sreenivasulu and N. Bhaskar Reddy

Department of Mathematics, Sri Venkateswara University, Tirupati-517502, India.

ARTICLE INFO

Article history:

Received: 18 August 2012;

Received in revised form:

30 September 2012;

Accepted: 4 October 2012;

Keywords

Thermal radiation,
Viscous dissipation,
Mixed convection,
Boundary layer flow,
Exponentially stretching surface,
Soret and Dufour effects.

ABSTRACT

The Soret and Dufour effects of on mixed convection flow of a viscous incompressible radiating and dissipative fluid over an exponentially stretching vertical surface in a quiescent fluid is analyzed. Stretching velocity, wall temperature and wall concentrations are assumed to have specific exponential function forms. The governing system of partial differential equations is transformed into a system of ordinary differential equations using similarity transformations and then solved numerically using the Runge-Kutta fourth order technique along with shooting method. The effects of the various parameters on the velocity, temperature and concentration profiles are illustrated in graphically.

Introduction

The boundary layer flow on a continuous stretching sheet has attracted considerable attention during the last few decades due to its numerous applications in industrial manufacturing processes such as hot rolling, wire drawing, glass-fiber and paper production, drawing of plastic films, metal and polymer extrusion and metal spinning. Both the kinematics of stretching and the simultaneous heating or cooling during such processes has a decisive influence on the quality of the final products (Magyari & Keller [1]).

Crane [2] was the first to consider the boundary layer flow caused by a stretching sheet which moves with a velocity varying linearly with the distance from a fixed point. The heat transfer aspect of this problem was investigated by Carragher and Crane [3], under the conditions when the temperature difference between the surface and the ambient fluid is proportional to a power of the distance from a fixed point. Magyari and Keller [1] investigated the steady boundary layers on an exponentially stretching continuous surface with an exponential temperature distribution.

In practical situations, the flow over a continuous material moving through a quiescent fluid is induced by the movement of the solid material and by thermal buoyancy. Therefore, these two mechanisms, surface motion and buoyancy force, will determine the momentum and thermal transport processes. The thermal buoyancy force arising due to the heating or cooling of a continuously moving surface, under some circumstances, may alter significantly the flow and thermal fields and thereby the heat transfer behavior in the manufacturing process. By considering the effect of buoyancy, Ali and Al-Yousef [4] analyzed mixed convection heat transfer from an uniformly stretching vertical surface with general power function form for stretching velocity of the wall and with surface suction/injection. Partha *et al.* [5] presented a similarity solution for mixed convection flow and heat transfer from an exponentially stretching surface by considering viscous dissipation effect in the medium. They showed that the buoyancy and viscous dissipation have significant influence on the non-dimensional skin friction and heat transfer coefficient. Recently, Dulal Pal [6] reported an analysis to describe mixed convection heat transfer in the boundary layers on an exponentially stretching continuous surface with an exponential temperature distribution in the presence of magnetic field, viscous dissipation and internal heat generation/absorption.

When heat and mass transfer occur simultaneously in a moving fluid, the relations between the fluxes and the driving potentials are of a more intricate nature. It has been observed that an energy flux can be generated not only by temperature gradients but also by concentration gradients. The energy flux caused by a concentration gradient is termed the diffusion-thermo (Dufour) effect. On the other hand, mass fluxes can also be created by temperature gradients and this embodies the thermal-diffusion (Soret) effect. In most of the studies related to heat and mass transfer process, Soret and Dufour effects are neglected on the basis that they are of a smaller order of magnitude than the effects described by Fourier's and Fick's laws. But these effects are considered as second order phenomena and may become significant in areas such as hydrology, petrology, geosciences, etc. The Soret effect, for instance, has been utilized for isotope separation and in mixture between gases with very light molecular weight and of medium molecular weight. The Dufour effect was found to be of order of considerable magnitude so that it cannot be neglected [Eckert and Drake[7]]. Dursunkaya and Worek[8] studied diffusion-thermo and thermal-diffusion effects in transient and steady natural convection from a vertical surface, whereas Kafoussias and Williams[9] presented the same effects on mixed convective and mass transfer steady laminar boundary layer flow over a vertical flat plate with temperature dependent viscosity.

Tele:
E-mail addresses: psreddysvu11@gmail.com

El-Aziz [10] investigated the combined effects of thermal-diffusion and diffusion-thermo on MHD heat and mass transfer over a permeable stretching surface with thermal radiation. Ahmed [11] discussed free convective heat and mass transfer of an incompressible, electrically conducting fluid over a stretching sheet in the presence of suction and injection with thermal-diffusion and diffusion-thermo effects. A study has been carried out to analyze the combined effects of Soret and Dufour on unsteady MHD non-Darcy mixed convection over a stretching sheet embedded in a saturated porous medium in the presence of thermal radiation, viscous dissipation and first-order chemical reaction by Pal and Mondal [12].

In physics and engineering, the radiative effects have important applications. In space technology and high temperature processes, knowledge of radiation heat transfer becomes very important for the design of pertinent equipment (Seddeek [13]). Hossain and Takhar [14], Takhar *et al.* [15], Hossain *et al.* [16] investigated the effect of radiation on heat transfer problems in detail. Recently, Sajid and Hayat [17] extended the problem of Partha *et al.* [5] by investigating the radiation effects on the flow over an exponentially stretching sheet, and solved the problem analytically using the homotopy analysis method. The numerical solution for the same problem was then given by Bidin and Nazar [18].

However, no attempt has been made to analyze the Soret and Dufour effects on boundary layer flow and radiative heat transfer over an exponential stretching surface in the presence of viscous dissipation, and hence it is considered in the present problem. Wall temperature, wall concentration and stretching velocity are assumed to have specific exponential function forms. The Runge-Kutta technique along with shooting method is employed to solve the non-linear system in the problem. The effects of mixed convection parameters, radiation parameter, Soret and Dufour numbers, Prandtl number, Eckert number, Schmidt number and also *X*- location are examined and are displayed through graphs. Also, the effects of skin friction, heat and mass transfer coefficient is illustrated in tabular form for various parameters. The results are compared with relevant results in the existing literature and are found to be in good agreement.

Mathematical Analysis

A steady, two-dimensional laminar flow of an incompressible viscous and radiating fluid near an impermeable vertical sheet stretching with velocity $u_w(x)$, temperature distribution $T_w(x)$ and concentration distribution $C_w(x)$ moving through a quiescent incompressible fluid of constant temperature T_∞ and concentration C_∞ is considered, in the presence of thermal diffusion (Soret) and diffusion-thermo (Dufour) effects. The *x*-axis is directed along the continuous stretching sheet and points in the direction of motion and *y*-axis is perpendicular to it. The schematic diagram of the problem is shown below.

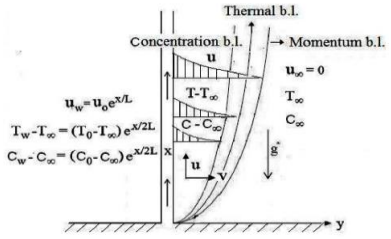

Figure 1: Physical model and coordinate system.

Now, under the usual Boussinesq's and boundary layer approximations, the governing equations for the flow field under consideration are

$$\frac{\partial u}{\partial x}+\frac{\partial v}{\partial y}=0 \tag{1}$$

$$u\frac{\partial u}{\partial x}+v\frac{\partial u}{\partial y}=\nu\frac{\partial^2 u}{\partial y^2}+g\beta(T-T_\infty)+g\beta^*(C-C_\infty) \tag{2}$$

$$u\frac{\partial T}{\partial x}+v\frac{\partial T}{\partial y}=\alpha\frac{\partial^2 T}{\partial y^2}-\frac{1}{\rho C_p}\frac{\partial q_r}{\partial y}+\frac{\nu}{C_p}\left(\frac{\partial u}{\partial y}\right)^2+\frac{DK_T}{C_s C_p}\frac{\partial^2 C}{\partial y^2} \tag{3}$$

$$u\frac{\partial C}{\partial x}+v\frac{\partial C}{\partial y}=D\frac{\partial^2 C}{\partial y^2}+\frac{DK_T}{T_m}\frac{\partial^2 T}{\partial y^2} \tag{4}$$

where, *x* and *y* are the coordinates along and perpendicular to the stretching sheet, *u* and *v* are the velocity components in the x and y directions, respectively, ν is the kinematic viscosity, β and β^* are the thermal and concentration expansion coefficients of the fluid respectively. *g* is the acceleration due to gravity, *T* is the temperature of the fluid, T_∞ is the temperature of the fluid far away from the plate, *C* is the concentration of the fluid, C_∞ is the species concentration of the fluid far away from the plate, q_r is the radiative heat flux. α is the thermal diffusivity, *D* is the solutal diffusivity of the medium, C_p is the specific heat capacity, C_s is the concentration susceptibility, T_m is the mean fluid temperature and K_T is the thermal diffusion ratio.

The second, third and fourth terms on the right-hand side of the energy equation (3) signifies the radiation, viscous dissipation and Dufour or diffusion-thermo effect respectively. The last term on the right-hand side of diffusion equation (4) signifies the Soret or thermal-diffusion effect.

The boundary conditions for the velocity, temperature and concentration fields are

$$u=u_w(x),\ v=0,\ T=T_w(x),\ C=C_w(x) \quad at \quad y=0$$
$$u\to 0,\quad T\to T_\infty,\quad C\to C_\infty \quad as \quad y\to\infty \tag{5}$$

where the subscripts *w* and ∞ indicate the conditions at the wall and at the outer edge of the boundary layer respectively.

The stretching velocity $u_w(x)$, exponential temperature distribution *c* and exponential concentration distribution $C_w(x)$ are defined as

$$u_w(x)=u_0 e^{x/L} \tag{6}$$

$$T_w(x)=T_\infty+(T_0-T_\infty)e^{x/2L} \tag{7}$$

$$C_w(x)=C_\infty+(C_0-C_\infty)e^{x/2L} \tag{8}$$

Where u_0 is velocity parameter of the stretching surface, T_0 is parameter of the temperature distribution where as C_0 is parameter of the concentration distribution in the stretching surface.

By employing Rosseland approximation (Sajid and Hayat[17]), the radiative heat flux q_r is given by

$$q_r=-\frac{4}{3}\frac{\sigma^*}{k^*}\frac{\partial T^4}{\partial \overline{y}} \tag{9}$$

where σ* is the Stefan-Boltzmann constant and *k** is the mean absorption coefficient. It should be noted that by using the Rosseland approximation, the present analysis is limited to optically thick fluids. If the temperature differences within the

flow field are sufficiently small, then equation (9) can be linearized by expanding T^4 into the Taylor series about T_∞, which after neglecting higher-order terms takes the form

$$T^4 \cong 4T_\infty^3 T - 3T_\infty^4 \tag{10}$$

In view of equations (9) and (10), equation (3) becomes

$$u\frac{\partial T}{\partial x} + v\frac{\partial T}{\partial y} = \alpha\left(1 + \frac{16\sigma^* T_\infty^3}{3K^* k}\right)\frac{\partial^2 T}{\partial y^2} + \frac{\nu}{C_p}\left(\frac{\partial u}{\partial y}\right)^2 + \frac{DK_T}{C_s C_p}\frac{\partial^2 C}{\partial y^2} \tag{11}$$

In view of the continuity equation (1), defining the stream function ψ such that

$$u = \frac{\partial \psi}{\partial y}, \qquad v = -\frac{\partial \psi}{\partial x} \tag{12}$$

In order to write the governing equations and the boundary conditions in dimensionless form, the following non-dimensional quantities are introduced.

$$\eta = \left(\frac{\mathrm{Re}}{2}\right)^{1/2}\frac{y}{L}e^{x/2L}, \qquad \psi = \sqrt{2}\nu\,\mathrm{Re}^{1/2}\,e^{x/2L} f(\eta),$$

$$T(x,y) = T_\infty + (T_0 - T_\infty)e^{x/2L}\theta(\eta), \quad C(x,y) = C_\infty + (C_0 - C_\infty)e^{x/2L}\phi(\eta),$$

$$X = \frac{x}{L}, \quad Ri = \frac{Gr}{\mathrm{Re}^2}, \quad N = \frac{\beta^*(C_0 - C_\infty)}{\beta(T_0 - T_\infty)}, \quad Nr = \frac{4\sigma^* T_\infty^3}{K^* k}, \quad \mathrm{Pr} = \frac{\nu}{\alpha},$$

$$E = \frac{u_0^2}{\rho(T_0 - T_\infty)}, \quad Sc = \frac{\nu}{D}, \quad D_u = \frac{DK_T(C_0 - C_\infty)}{C_s C_p(T_0 - T_\infty)}, \quad S_r = \frac{DK_T(T_0 - T_\infty)}{T_m \nu(C_0 - C_\infty)}. \tag{13}$$

In view of equations (12)-(13), the governing equations (2), (4) and (11) reduce to the dimensionless form

$$f''' + ff'' - 2(f')^2 + 2Ri\,e^{-3X/2}(\theta + N\phi) = 0 \tag{14}$$

$$\left(1 + \frac{4}{3}Nr\right)\theta'' + \mathrm{Pr}(f\theta' - f'\theta) + \mathrm{Pr}\,E\,e^{3X/2}(f'')^2 + \mathrm{Pr}\,D_u\phi'' = 0 \tag{15}$$

$$\phi'' + Sc(f\theta' - f'\theta) + ScSr\theta'' = 0 \tag{16}$$

The corresponding boundary conditions are

$$f(0) = 0, \quad f'(0) = 1, \quad \theta(0) = 1, \quad \phi(0) = 1,$$
$$f'(\eta) \to 0 \quad \theta(\eta) \to 0, \quad \phi(\eta) \to 0 \quad as \quad \eta \to \infty \tag{17}$$

where primes denotes the ordinary differentiation with respect to η, *L* is the characteristic length of the plate, *X* is the *X*-location, *Ri* is the mixed convection parameter, *N* is the buoyancy ratio, *Nr* is the radiation parameter, *Pr* is the Prandtl number, *E* is the Eckert number, *Sc* is the Schmidt number, D_u is the Dufour number and *Sr* is the Soret number.

A close look at the equations (14) and (15) reveals that, in mixed convection due to viscous fluid, the velocity and temperature profiles are not similar because the x-coordinate cannot be eliminated from those equations. Although local non-similarity solutions have been found for some boundary layer flows dealing with viscous fluid, the technique is hard to extend to in this case. Thus, for ease of analysis, it was decided to proceed with finding local similarity solutions for the governing equations (14) and (15). That is, taking *X* = x/L and then one can still study the effects of various parameters on different profiles at any given *X*- location.

The wall shear stress, heat and mass transfers acting on the surface in contact with the ambient fluid of constant density are respectively given by

$$\tau_w = \mu\left[\frac{\partial u}{\partial y}\right]_{y=0}, \quad q_w(x) = -k\left[\frac{\partial T}{\partial y}\right]_{y=0}, \quad q_m(x) = -D\left[\frac{\partial C}{\partial y}\right]_{y=0} \tag{18}$$

where μ is the dynamic viscosity.

The skin friction at the plate can be obtained, which in non-dimensional form is given by

$$C_f = \frac{2\tau_w}{\rho U_*^2} \qquad \Rightarrow C_f\,\mathrm{Re}_x^{1/2} = \sqrt{2x}\,f''(0) \tag{19}$$

The rate of heat transfer coefficient can be obtained, which in the non-dimensional form, in terms of the Nusselt number, is given by

$$Nu_x = \frac{x\,q_w(x)}{k(T_w(x) - T_\infty)} \quad \Rightarrow Nu_x\,\mathrm{Re}_x^{-1/2} = -\sqrt{\frac{X}{2}}\theta'(0) \tag{20}$$

The rate of mass transfer coefficient can be obtained, which in the non-dimensional form, in terms of the Sherwood number, is given by

$$Sh_x = \frac{x\,q_m}{D(C_w(x) - C_\infty)} \quad \Rightarrow Sh_x\,\mathrm{Re}_x^{-1} = -\sqrt{\frac{X}{2}}\phi'(0) \tag{21}$$

where $Re_x = u_w(x)\,x/\nu$ is the local Reynolds number.

Solution of the Problem

The governing boundary layer equations (14) – (16) subject to the boundary conditions (17) are solved numerically by using Runge-Kutta fourth order technique along with shooting method. First of all higher order non- linear differential equations (14) – (16) are converted into simultaneous linear differential equations of first order and they are further transformed into initial value problem by applying the shooting technique (Jain *et al.*[20]). The resultant initial value problem is solved by employing Runge-Kutta fourth order technique. The step size $\Delta\eta = 0.01$ is used to obtain the numerical solution with five decimal place accuracy as the criterion of convergence. From the process of numerical computation, the skin-friction coefficient, the Nusselt number and the Sherwood number which are respectively proportional to $f''(0)$, $-\theta'(0)$ and $-\phi'(0)$ are also sorted out and their numerical values are presented in a tabular form.

Results and Discussion

In order to get a physical insight into the problem, a representative set of numerical results is shown graphically in Figs.2-22, to illustrate the influence of physical parameters viz., the mixed convection parameter *Ri*, the buoyancy ratio *N*, the Prandtl number *Pr*, the radiation parameter *Nr*, the Eckert number *E*, the Schmidt number *Sc*, Dufour number (*Du*) and Soret number (*Sr*) on the velocity $f'(\eta)$, temperature $\theta(\eta)$ and concentration $\phi(\eta)$.

In the absence of mixed convection parameter *Ri*, Soret number *Sr* and Dufour number *Du*, Eckert number *E*, radiation parameter *Nr* with *N* = 0 and *Sc* = 0 for different values of the Prandtl number *Pr*, the results have been compared with the special case of Magyari and Keller [1] and found that they are in good agreement, as shown in Table 1.

In the present study, the following default parameter values are adopted for the numerical computations: *N* = 0.5, *Du* = 0.03, *Sr* = 2.0, *Ri* = 1, *Sc* = 0.22, *Pr* = 1.0, *X* = 0.5,*Nr* = 1.0 and *E* = 0.5. These values are used throughout the computations, unless otherwise indicated. Figs.2, 3 and 4 show the effects of the *X*-location on the dimensionless velocity, temperature and concentration. From Fig.2, it is noticed that the velocity decreases with an increase in the value of *X* in the momentum boundary layer. It is clear from Fig.3 that the thermal boundary layer thickness increases with the increase of *X* but with significant effect near the stretching sheet. It can be seen from Fig.4 that the solutal boundary layer thickness of the fluid

increases with the increase of *X* and also, found that significant effect within the boundary layer.

Figs.5, 6 and 7 depict the dimensionless velocity, temperature and concentration profiles for various values of the mixed convection parameter *Ri.* Also, we have analyzed the results for both cases of aiding and opposing flows. It reveals that as the value of *Ri* increases, the dimensionless velocity rises. Compared with the limiting case of *Ri* = 0.0 (i.e., pure forced convection), the velocity is more for aiding flow and the velocity is less for opposing flow. As *Ri* increases, the buoyancy effects increase and hence the fluid flow accelerates. Fig.6 illustrates the dimensionless temperature for different values of *Ri.* The results indicate that the dimensionless temperature reduces with the increase of *Ri.* The temperature in case of mixed convection is less for aiding flow and more for opposing flow compared to that of pure forced convection. As *Ri* (i.e. buoyancy effects) increases, the convection cooling effect increases and hence the temperature reduces. The effect of mixed convection parameter *Ri* on the dimensionless concentration is depicted in Fig.7. It is clear that the concentration of the fluid decreases with the increase of mixed convection parameter *Ri*. Fig. 8 shows the velocity profiles for different values of buoyancy ratio parameter *N*. It is seen that the velocity increases with an increase in buoyancy ratio parameter.

The effects of the *Pr* on the dimensionless velocity, temperature and concentration are depicted in the Figs.9-11. *Pr* encapsulates the ratio of momentum diffusivity to thermal diffusivity. Larger *Pr* values imply a thinner thermal boundary layer thickness and more uniform temperature distributions across the boundary layer. Hence the thermal boundary layer will be much less in thickness than the hydrodynamic boundary layer. *Pr* = 1 implies that the thermal and velocity boundary layers are approximately equal. Smaller *Pr* fluids have higher thermal conductivities so that heat can diffuse away from the vertical plate faster than for higher *Pr* fluids (thicker boundary layers). As *Pr* enhances, it can be seen from Fig.9 that the velocity reduces since the fluid is increasingly viscous as *Pr* rises. Hence the viscous fluid is decelerated with a rise in *Pr*. Fig.10 indicates that a rise in *Pr* substantially reduces the temperature in the viscous fluid. From Fig.11 it is found that the solutal boundary layer thickness of the fluid enhances with the enhance of *Pr*.

The influence of thermal radiation parameter *Nr* on the velocity, temperature and concentration are shown in Figs.12-14. The radiation parameter *Nr* defines the relative contribution of conduction heat transfer to thermal radiation transfer. It is obvious that an increase in the radiation parameter results in increasing both the velocity and temperature while the concentration of the fluid decreases within the boundary layer.

Figs.15, 16 and 17 represent the dimensionless velocity, temperature and concentration profiles for various values of the viscous dissipation parameter i.e., the Eckert number *E*. The Eckert number *E* expresses the relationship between the kinetic energy in the flow and the enthalpy. It embodies the conservation of kinetic energy into internal energy by work done against the viscous fluid stress. The positive Eckert number implies cooling of the sheet i.e., loss of heat from the sheet to the fluid. It is found that as E increases, both the velocity as well as the temperature increases while the concentration decreases.

For different values of the Schmidt number *Sc*, the velocity and concentration profiles are plotted in Figs. 18 and 19. The Schmidt number *Sc* embodies the ratio of momentum diffusivity to the mass (species) diffusivity. It physically relates the relative thickness of the hydrodynamic boundary layer and mass transfer (concentration) boundary layer. As the Schmidt number increases the concentration decreases. This causes the concentration buoyancy effects to decrease, yielding a reduction in the fluid velocity. The reduction in the velocity and concentration profiles is accompanied by simultaneous reductions in the velocity and concentration boundary layers, which is evident from Figs. 18 and 19.

The effects of Soret (*Sr)* and Dufour (*Du)* numbers on the velocity, temperature and concentration profiles are depicted in Figs.20-22. The velocity as well as temperature increases but the concentration decreases with a decrease in the Soret number *Sr* (or simultaneous increase in the Dufour number *Du*) more effectively near the surface of the stretching sheet. Thus it is concluded from Figs.20-22 that the velocity, temperature and concentration distributions are severely affected by the Soret and Dufour effects, especially the thermal boundary layer thickness which increases while concentration boundary layer thickness which decreases with increase in the Dufour number (or simultaneously decrease in the Soret number). It should be mentioned that the profiles of concentration are found to be more sensible to the changes with Soret number *Sr* and Dufour number *Du*, respectively. Thus it is evident that the effects are obviously playing an important role under mixed convection flow for molecular diffusion in the presence of Soret and Dufour effects. Therefore, we can understand that the influence of thermal-diffusion as well as the diffusion- thermal effects is greatly effective in the study of mixed convection problems.

The variations of $f''(0)$, $-\theta'(0)$ and $-\phi'(0)$ which are proportional to the local skin-friction coefficient, rate of heat and mass transfers are shown in Table.2 for different values of the mixed convection parameter *Ri*, in both cases of opposing and aiding flows. It is seen that the local skin friction factor increases as *Ri* increases. The reason is that an increase in the buoyancy effect in mixed convection flow leads to an acceleration of the fluid flow, which increases the local skin friction factor. It is also seen that, the heat transfer rate increases but the mass transfer rate decreases in both cases of opposing and aiding flows with the increasing values of *Ri*. It is also found from Table.2 that the skin friction, heat transfer coefficient are reducing and the mass transfer coefficient is increasing with the increasing values of *X*-location. The effect of increasing the value of *Pr* is to decrease the skin friction and mass transfer coefficients but increases heat transfer coefficient. The effect of increasing the value of *Nr* is to increase the skin friction and mass transfer coefficients but decreases heat transfer coefficient. The effect of increasing the value of *E* is to increase the skin friction and mass transfer coefficients but decreases heat transfer coefficient. Finally, the effects of Dufour and Soret number on the local skin-friction coefficient and the rate of heat and mass transfers are shown in this table. The behavior of these parameters is self-evident from the Table.2 and hence is not discussed for brevity.

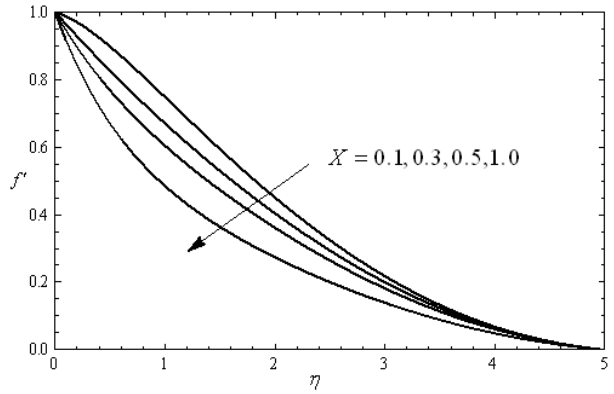

Fig.2. Velocity profiles for different values of *X*

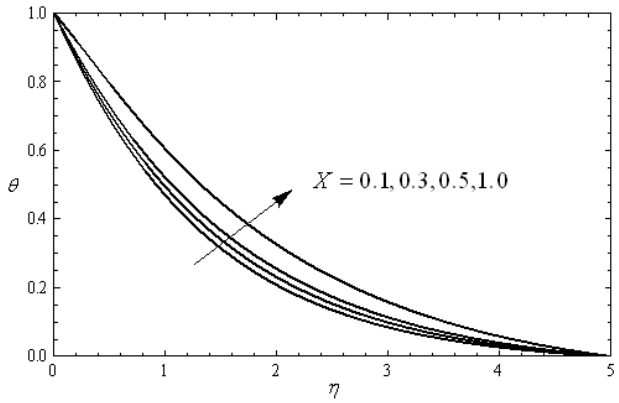

Fig.3. Temperature profiles for different values of X

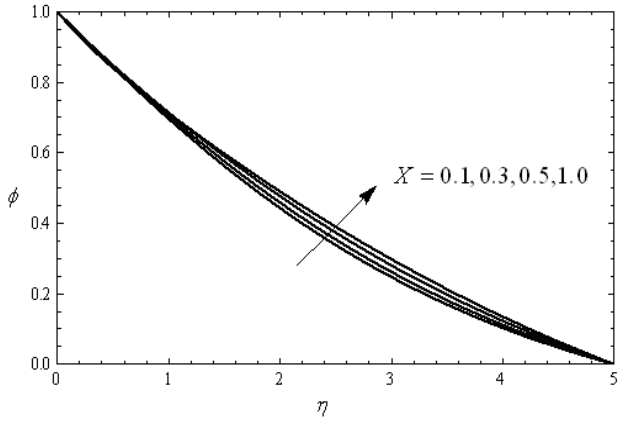

Fig.4. Concentration profiles for different values of X

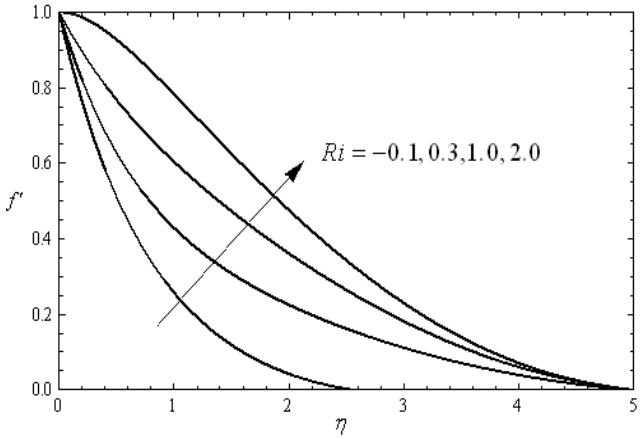

Fig.5. Velocity profiles for different values of *Ri*

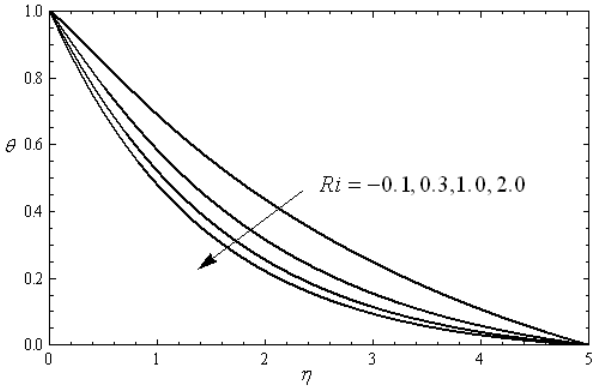

Fig.6. Temperature profiles for different values of *Ri*

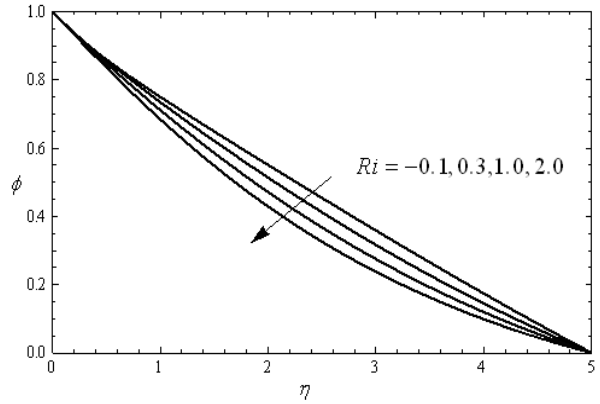

Fig.7. Concentration profiles for different values of *Ri*

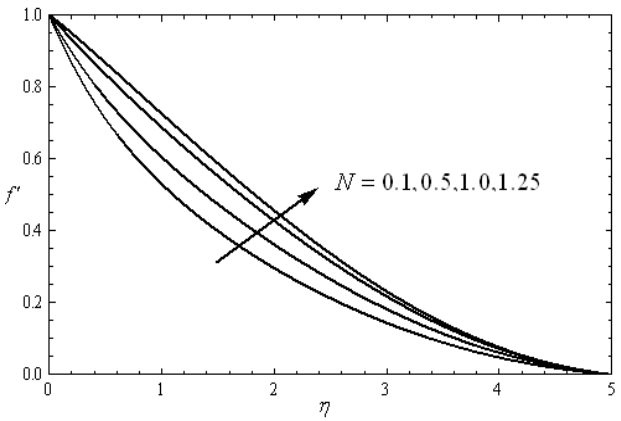

Fig.8. Velocity profiles for different values of *N*

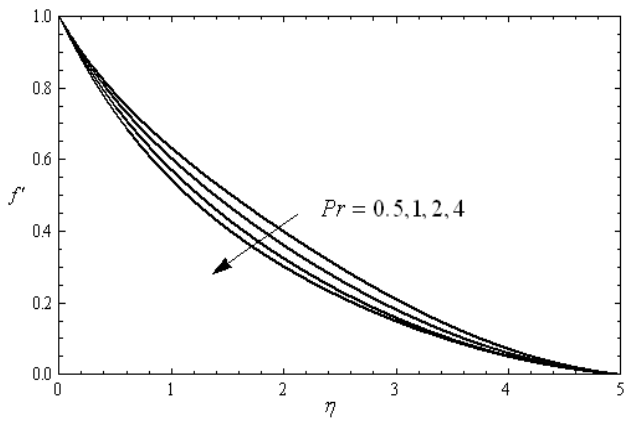

Fig.9. Velocity profiles for different values of *Pr*

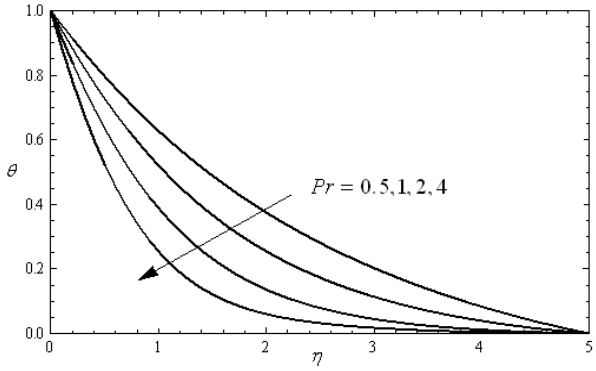

Fig.10. Temperature profiles for different values of *Pr*

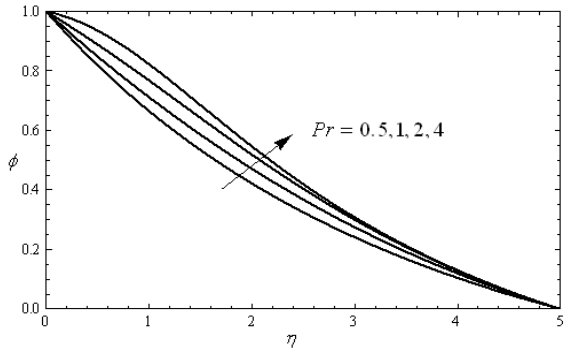

Fig.11. Concentration profiles for different values of *Pr*

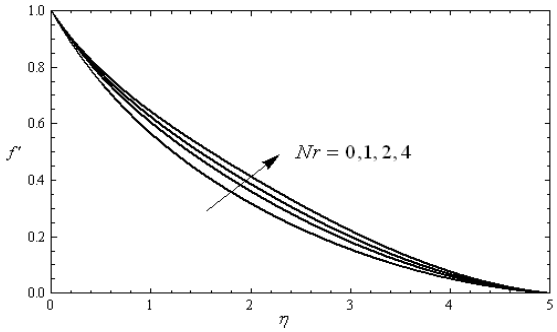

Fig.12. Velocity profiles for different values of *Nr*

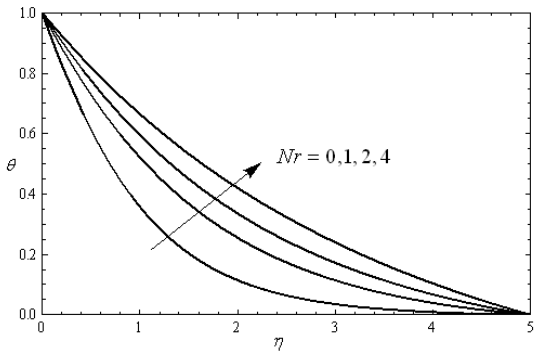

Fig.13. Temperature profiles for different values of *Nr*

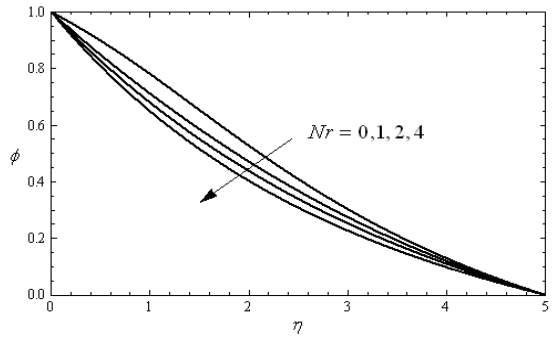

Fig.14. Concentration profiles for different values of *Nr*

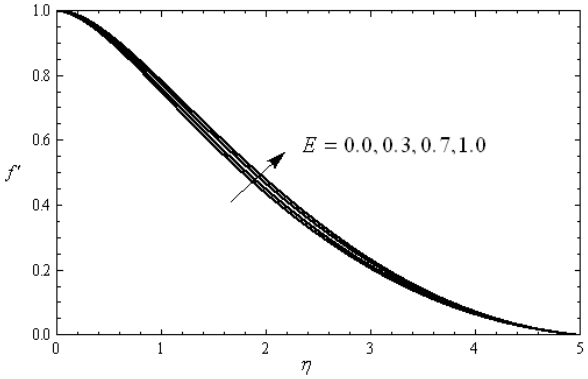

Fig.15. Velocity profiles for different values of *E*

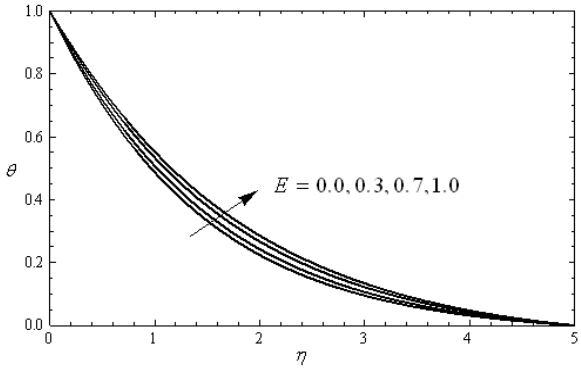

Fig.16. Temperature profiles for different values of *E*

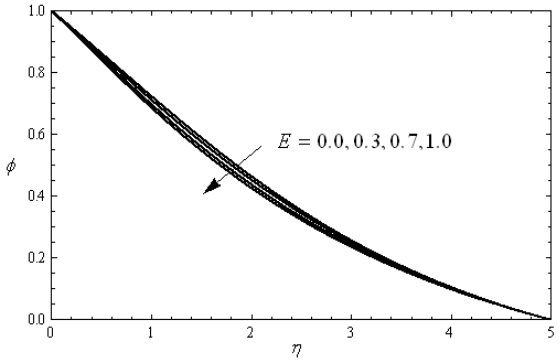

Fig.17. Concentration profiles for different values of *E*

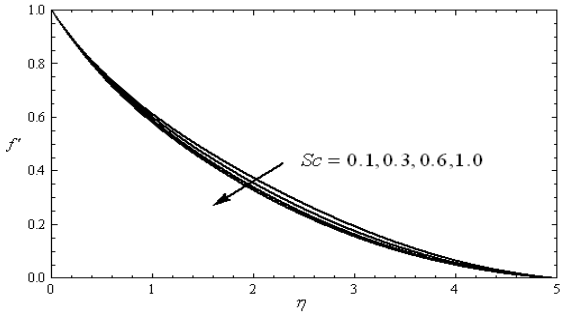

Fig.18. Velocity profiles for different values of *Sc*

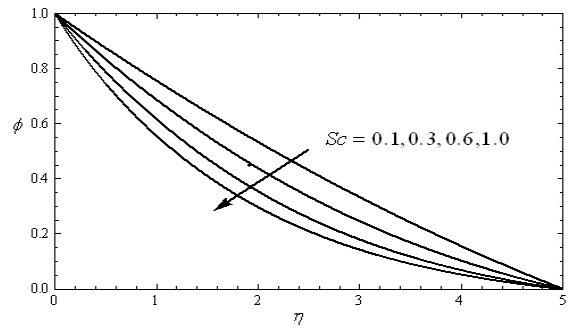

Fig.19. Concentration profiles for different values of *Sc*

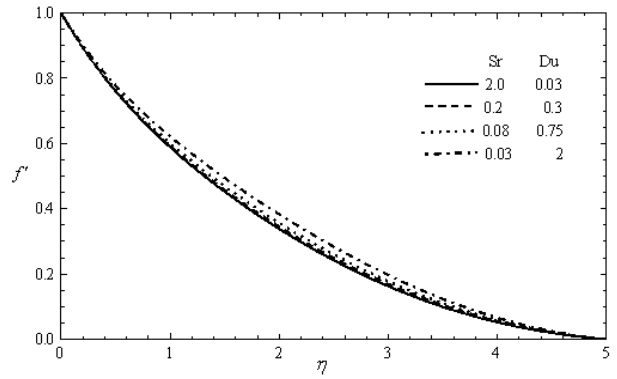

Fig.20. Velocity profiles for different values of *Sr* and *Du*

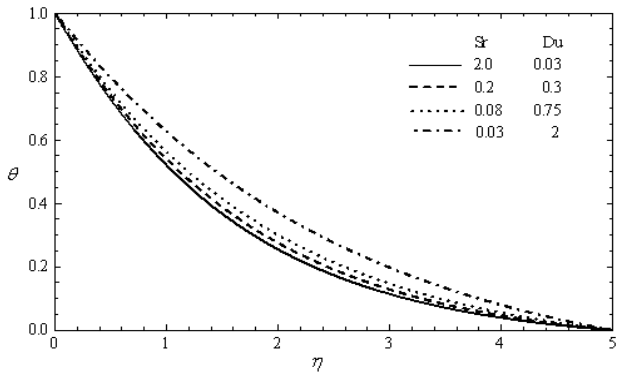

Fig.21. Temperature profiles for different values of *Sr* and *Du*

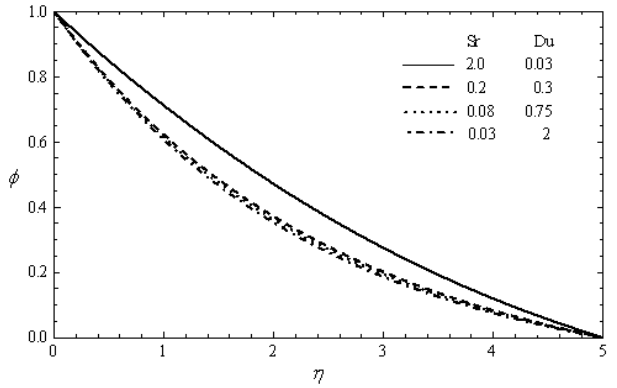

Fig.22. Concentration profiles for different values of *Sr* and *Du*

Conclusions

The present study gives numerical solutions for the Soret and Dufour effects on mixed convection heat and mass transfer in a viscous fluid over an exponentially stretching vertical surface in the presence of thermal radiation and viscous dissipation. Using the similarity variables, the governing equations are transformed into a set of ordinary differential equations where numerical solution has been presented for different values of parameters. The present results are found to be in excellent agreement with previously published work on various special cases of the problem.

1. An increase in the mixed convection parameter *Ri*, enhances the velocity, skin friction and heat transfer coefficient but reduces the temperature, concentration distributions and mass transfer coefficient, in the boundary layer.
2. The velocity, skin friction as well as the rate of heat transfer decrease whereas the wall temperature, wall concentration and rate of mass transfer increase with an increase in *X*, in the boundary layer.
3. Increasing the Prandtl number substantially decreases the velocity, temperature, skin friction and mass transfer rate where as increases the concentration and rate of heat transfer.
4. The velocity, temperature and local mass transfer rate increases whereas the concentration, skin-friction and local heat transfer rate decrease with an increase in the Dufour number (or simultaneous decrease in the Soret number).
5. The velocity, temperature as well as skin friction and mass transfer rate increases whereas the concentration and local heat transfer rate decreases with an increase in the radiation parameter or Eckert number.

References

[1] Magyari, E. and Keller, B. Heat and mass transfer in the boundary layers on an exponentially stretching continuous surface. *J. Phys. D: Appl. Phys.* 32(1999), 577-585.

[2] Crane, L.J. Flow past a stretching plate. *Z. Angew. Math. Phys.* 21(1970), 645-655.

[3] Carragher, P. and Crane, L.J. Heat transfer on a continuous stretching sheet. *Z. Angew. Math. Mech.* 62(1982), 564-573.

[4] M.E. Ali and F. Al-Youself. Laminar mixed convection boundary layers induced by a linearly stretching permeable surface. *Int. J. Heat Mass Transfer* 45(2002), 4241-4250.

[5] M.K. Partha, P.V.S.N. Murthy and G.P. Rajasekhar. Effect of viscous dissipation on the mixed convection heat transfer from an exponentially stretching surface. *Heat Mass Transfer* 41(2005), 360-366.

[6] Dulal Pal. Mixed convection heat transfer in the boundary layers on an exponentially stretching surface with magnetic field. *Applied Mathematics and Computation* 217(2010), 2356-2369.

[7] E.R.G. Eckeret and R.M. Drake: Analysis of heat and mass transfer. *McGraw Hill, Newyark* (1972).

[8] Z. Dursunkaya and WMWorek: Diffusion-thermo and thermal diffusion effects in transient and steady natural convection from a vertical surface. *Int. J. Heat Mass Transfer* 35(1992), 2060- 2065.

[9] N.G. Kafoussias and N.G. Williams: Thermal-diffusion and diffusion-thermo effects on mixed free-forced convective and mass transfer boundary layer flow with temperature dependent viscosity. *Int. J. Engng. Sci.* 33(1995), 1369-1384.

[10] M.A. El-Aziz. Thermal-diffusion and diffusion-thermo effects on combined heat mass transfer by hydromagnetic three-dimensional free convection over a permeable stretching surface with radiation. *Physics Letter A*372 (2008), 263-272.

[11] A.A. Ahmed. Similarity solution in MHD: Effects of thermal diffusion and diffusion thermo on free convective heat and mass transfer over a stretching surface considering suction or injection. *Commun Nonlinear Sci. Numer. Simulat.*14 (2009), 2202-2214.

[12] D. Pal and H. Mondal. Effects of Soret Dufour, chemical reaction and thermal radiation on MHD non-Darcy unsteady mixed convective heat and mass transfer over a stretching sheet. *Commun Nonlinear Sci. Numer. Simulat.*16 (2011), 1942-1958.

[13] Seddeek M.A. Effects of radiation and variable viscosity on a MHD free convection flow past a semi-infinite flat plate with an aligned magnetic field in the case of unsteady flow. *Int. J. Heat Mass Transfer* 45(2002), 931-935.

[14] Hossain M.A. and Takhar H.S. Radiation effect on mixed convection along a vertical plate with uniform surface temperature. *Int J Heat Mass Transf* 31(1996), 243–248.

[15] Takhar H.S., Gorla R.S.R. and Soundalgekar V.M. Radiation effects on MHD free convection flow of a gas past a

semi-infinite vertical plate. *Int J Numer Meth Heat Fluid Flow* 6(2) (1996), 77–83.
[16] Hossain M.A., Alim M.A. and Rees D.A. The effect of radiation on free convection from a porous vertical plate. *Int J Heat Mass Transf* 42(1999), 181–191.
[17] Sajid, M. and Hayat, T. Influence of thermal radiation on the boundary layer flow due to an exponentially stretching sheet. *Int. Comm. Heat Mass Transfer* 35(2008), 347-356.
[18] Bidin, B. and Nazar, R. Numerical solution of the boundary layer flow over an exponentially stretching sheet with thermal radiation. *Euro J. Sci. Res*. 33(4) (2009), 710-717.
[19] Srinivasacharya D. and RamReddy Ch. Soret and Dufour effects on mixed convection from an exponentially stretching surface. *International Journal of Nonlinear Science.* 12(2011), pp.60-68.
[20] Jain M.K., Iyengar S.R.K. and Jain R.K (1985), Numerical methods for Specific and Engineering Computation, Wiley Eastern Ltd., New Delhi, India.

Table 1 Comparison between wall-temperature gradient θ′(0) calculated by the present method and that of Srinivasacharya and RamReddy[19] and Magyari and Keller[1] for *Ri= Sr=Nr=E = Du=N = 0* and *Sc* = 0.

Pr	Present Results	Srinivasacharya and RamReddy[19]	Magyari and Keller[1]
0.5	-0.595283	-0.59438	-0.59434
1.0	-0.954787	-0.95478	-0.95478
3.0	-1.86907	-1.86908	-1.86908
5.0	-2.50013	-2.50015	-2.50014
8.0	-3.24212	-3.24218	-3.24213
10	-3.66035	-3.66043	-3.66038

Table 2 Effects of the skin friction, heat and mass transfer coefficients for different values of *Ri, Sr, Du, X, Pr, Nr* and *E*.

Ri	*Sr*	*Du*	*X*	*Pr*	*Nr*	*E*	$f''(0)$	$-\theta'(0)$	$-\phi'(0)$
-0.5	2.0	0.03	3.0	1.0	1.0	0.5	-1.334486	-9.3641	4.60201
-0.1	2.0	0.03	3.0	1.0	1.0	0.5	-1.32173	-9.11273	4.41678
0.5	2.0	0.03	3.0	1.0	1.0	0.5	-1.30236	-8.76008	4.18648
3.0	2.0	0.03	3.0	1.0	1.0	0.5	-1.22532	-7.52601	3.51594
5.0	2.0	0.03	3.0	1.0	1.0	0.5	-1.16726	-6.72932	3.13997
1.0	2.0	0.03	0.5	1.0	1.0	0.5	-0.723998	0.611368	0.322673
1.0	1.6	0.04	0.5	1.0	1.0	0.5	-0.724804	0.609762	0.354640
1.0	1.0	0.06	0.5	1.0	1.0	0.5	-0.725949	0.606792	0.402041
1.0	0.5	0.12	0.5	1.0	1.0	0.5	-0.726564	0.601234	0.441319
1.0	0.1	0.6	0.5	1.0	1.0	0.5	-0.728640	0.565303	0.474524
1.0	2.0	0.03	0.1	1.0	1.0	0.5	-0.282449	0.718307	0.313646
1.0	2.0	0.03	0.5	1.0	1.0	0.5	-0.723998	0.611368	0.322673
1.0	2.0	0.03	1.0	1.0	1.0	0.5	-1.02178	0.363386	0.384924
1.0	2.0	0.03	2.0	1.0	1.0	0.5	-1.23730	-1.25096	1.015330
1.0	2.0	0.03	3.0	1.0	1.0	0.5	-1.28649	-8.48566	4.023110
1.0	2.0	0.03	0.5	0.5	1.0	0.5	-0.716085	0.485088	0.397694
1.0	2.0	0.03	0.5	1.0	1.0	0.5	-0.723998	0.611368	0.322673
1.0	2.0	0.03	0.5	2.0	1.0	0.5	-0.737395	0.814163	0.216231
1.0	2.0	0.03	0.5	3.0	1.0	0.5	-0.748265	0.974549	0.138298
1.0	2.0	0.03	0.5	5.0	1.0	0.5	-0.764720	1.223770	0.020739
1.0	2.0	0.03	0.5	1.0	0.5	0.5	-0.729710	0.699084	0.275062
1.0	2.0	0.03	0.5	1.0	1.0	0.5	-0.723998	0.611368	0.322673
1.0	2.0	0.03	0.5	1.0	2.0	0.5	-0.718336	0.521679	0.374976
1.0	2.0	0.03	0.5	1.0	3.0	0.5	-0.715524	0.475867	0.403570
1.0	2.0	0.03	0.5	1.0	5.0	0.5	-0.712725	0.429278	0.434316
1.0	2.0	0.03	0.5	1.0	1.0	0.1	-0.734893	0.689806	0.295862
1.0	2.0	0.03	0.5	1.0	1.0	0.5	-0.723998	0.611368	0.322673
1.0	2.0	0.03	0.5	1.0	1.0	1.0	-0.710615	0.518347	0.354283
1.0	2.0	0.03	0.5	1.0	1.0	2.0	-0.684577	0.347722	0.411741
1.0	2.0	0.03	0.5	1.0	1.0	3.0	-0.659421	0.195592	0.462406